Title

Geometrical splitting technique to improve the computational efficiency in Monte Carlo calculations for proton therapy

Journal

Medical Physics, 40(4)

ISSN

0094-2405

Authors

Ramos-Méndez, José
Perl, Joseph
Faddegon, Bruce
et al.

Publication Date

2013-03-20

DOI

10.1118/1.4795343

Peer reviewed

Geometrical splitting technique to improve the computational efficiency in Monte Carlo calculations for proton therapy

José Ramos-Méndez[a)]
Benemérita Universidad Autónoma de Puebla, 18 Sur and San Claudio Avenue, Puebla, Puebla 72750, Mexico

Joseph Perl
SLAC National Accelerator Laboratory, 2575 Sand Hill Road, Menlo Park, California 94025

Bruce Faddegon
Department of Radiation Oncology, University of California at San Francisco, California 94143

Jan Schümann and Harald Paganetti
Department of Radiation Oncology, Massachusetts General Hospital and Harvard Medical School, Boston, Massachusetts 02114

(Received 26 July 2012; revised 1 February 2013; accepted for publication 28 February 2013; published 20 March 2013)

Purpose: To present the implementation and validation of a geometrical based variance reduction technique for the calculation of phase space data for proton therapy dose calculation.
Methods: The treatment heads at the Francis H Burr Proton Therapy Center were modeled with a new Monte Carlo tool (TOPAS based on Geant4). For variance reduction purposes, two particle-splitting planes were implemented. First, the particles were split upstream of the second scatterer or at the second ionization chamber. Then, particles reaching another plane immediately upstream of the field specific aperture were split again. In each case, particles were split by a factor of 8. At the second ionization chamber and at the latter plane, the cylindrical symmetry of the proton beam was exploited to position the split particles at randomly spaced locations rotated around the beam axis. Phase space data in IAEA format were recorded at the treatment head exit and the computational efficiency was calculated. Depth–dose curves and beam profiles were analyzed. Dose distributions were compared for a voxelized water phantom for different treatment fields for both the reference and optimized simulations. In addition, dose in two patients was simulated with and without particle splitting to compare the efficiency and accuracy of the technique.
Results: A normalized computational efficiency gain of a factor of 10–20.3 was reached for phase space calculations for the different treatment head options simulated. Depth–dose curves and beam profiles were in reasonable agreement with the simulation done without splitting: within 1% for depth–dose with an average difference of (0.2 ± 0.4)%, 1 standard deviation, and a 0.3% statistical uncertainty of the simulations in the high dose region; 1.6% for planar fluence with an average difference of (0.4 ± 0.5)% and a statistical uncertainty of 0.3% in the high fluence region. The percentage differences between dose distributions in water for simulations done with and without particle splitting were within the accepted clinical tolerance of 2%, with a 0.4% statistical uncertainty. For the two patient geometries considered, head and prostate, the efficiency gain was 20.9 and 14.7, respectively, with the percentages of voxels with gamma indices lower than unity 98.9% and 99.7%, respectively, using 2% and 2 mm criteria.
Conclusions: The authors have implemented an efficient variance reduction technique with significant speed improvements for proton Monte Carlo simulations. The method can be transferred to other codes and other treatment heads. © *2013 American Association of Physicists in Medicine*. [http://dx.doi.org/10.1118/1.4795343]

Key words: Monte Carlo, variance reduction, proton therapy, TOPAS, treatment head

I. INTRODUCTION

The aim of any radiotherapy treatment is to deliver high dose to the tumor while sparing healthy tissue.[1] Compared with conventional radiotherapy techniques, proton therapy often reaches higher conformity due to its dosimetric advantages, such as lack of exit dose and reduction of the total energy deposited in the patient (integral dose). The accuracy of treatment planning requires the use of sophisticated and fast dose calculation methods.

The Monte Carlo method, capable of handling complex geometries with full consideration of detailed physical processes, has become the gold standard for dose calculation in conventional radiotherapy.[2] However, due in part to the long computational time taken by Monte Carlo simulations to reach the clinically desirable statistical uncertainty (using terminology from Ref. 2), they are not fully employed in clinical practice. Variance reduction techniques (VRT) have been used in conventional radiotherapy calculations to reduce the simulation time to a more clinically practical level.[3–8] The

aim of a VRT in conventional radiotherapy is to increase the number of rare events of interest (e.g., the frequency of bremsstrahlung) or the secondary particles produced in these events, without adding systematic errors.[9] As a result, the simulation time to produce these events is reduced while maintaining unbiased results. The particle splitting technique and Russian roulette are commonly used VRT's in conventional radiotherapy.[3,4,8,10–12] For example, in directional bremsstrahlung splitting with Russian roulette, once an electron undergoes a bremsstrahlung process the resulting photon is split into N photons of different energies and directions, with N a user-defined number. The statistical weights of the new photons are decreased by a factor of $1/N$. Subsequently the direction of each new photon is calculated and if aimed into the field of interest, it is kept. If not, Russian roulette is played on the photon. Other physical effects can also be split (Compton effect, pair annihilation, pair creation, and photoelectric effect).[10] Particle splitting can also be implemented by geometrical considerations and is often used in shielding design simulations.[13,14] The simplest method is to divide the entire geometry into geometric cells and to assign to the cell$_i$ an importance value C_i. When a particle of interest travels from the cell$_i$ to the cell$_{i+1}$, if the ratio $r = C_{i+1}/C_i$ is larger than 1, then the particle is split into r new particles with statistical weights adjusted to $1/r$. If the ratio r is less than 1, Russian roulette is played on the particle with a probability of survival of $1 - r$. A width of the cells of the order of the distance between collisions of interest is recommended, and typical importance values for radiotherapy are $2^{[i]}$, with $i = 0, 1 \ldots k$.[7] On other hand, the more sophisticated weight window technique combines the geometry of the experiment and the energy of the particle to provide decreased simulation time compared to geometry splitting for most problems.[15,16] In this technique a minimum and maximum weight value is defined and particles with weight between these values are split and their weight adjusted. The implementation is more difficult than considering only the geometry, and sometimes the configuration is generated automatically by software.[17]

While in radiation therapy most VRT's have been applied for photon Monte Carlo applications, proton treatment planning could likewise benefit from implementing VRT's. VRT's for Monte Carlo simulation of conventional radiotherapy cannot generally be directly applied to passive scattered proton therapy due to fundamental differences of the relevant physics. In passive scattered proton therapy, the particles of interest at the treatment nozzle are the primary and secondary protons,[18] and the most frequent events include collisional energy losses and multiple Coulomb scattering.[1] Particle splitting for these processes is computationally impractical because of the extremely high number of collisions in a single volume. Geometry-based VRT as generally used in conventional radiotherapy also becomes impractical because the very low distance between collisions implies a high number of cells, and the importance values of cells located near the scoring region can reach many orders of magnitude. The weight window technique is a suitable alternative, but seems to be of limited value in terms of efficiency gain.[19,20]

Several efforts have been made to reduce the simulation time in Monte Carlo dose calculation for proton therapy, developing simplified Monte Carlo or hybrid analytical Monte Carlo algorithms[19,21–23] or GPU based algorithms.[24] However, these approaches do not consider the tracking of protons through the treatment head. Because treatment head geometries in passive scattered proton therapy strongly depend on the field, i.e., the tumor shape and location, the full treatment head in proton therapy is best simulated explicitly when using Monte Carlo for dose calculation.[25] In a typical scenario more than half of the calculation time is spent tracking particles through the treatment head as compared to the patient.[26] Therefore, VRT techniques that can reduce tracking of unnecessary particles through the treatment head become attractive in proton therapy. To our knowledge the current VRT's applied to proton therapy only consider the study of the penumbra effect caused by scattered protons in pencil beams[27,28] or shielding simulations for assessing the deposited dose of secondary neutrons.[29] A weight window technique implementation of VRT's for nozzle simulations only reduced the simulation time by a factor of 2 in MCNPX.[19,20] Very little information is available regarding the quantification of computational efficiency gains when using VRT's in the most common application of Monte Carlo simulation in proton therapy:[25,26,30,31] the production of phase space data (PHSP).

In this work, the well accepted particle-splitting and Russian roulette techniques[3,4,7,8] have been adapted to the specific needs of proton therapy in passive scattering mode and implemented in a recently developed Monte Carlo Tool for Particle Simulation, TOPAS.[32–34] This tool was then used for modeling the gantry mounted treatment heads at the Francis H Burr Proton Therapy Center (FHBPTC) at Massachusetts General Hospital (MGH). The study of the influence of computational efficiency by considering particle-splitting and Russian roulette for the production of PHSP was considered. Finally, dose distributions in a water phantom and in two patients geometries were calculated and compared with reference data.

II. MATERIALS AND METHODS

II.A. The TOPAS code

TOPAS is under development at SLAC National Accelerator Laboratory, the Massachusetts General Hospital and the University of California San Francisco. Building on top of the Geant4 toolkit, TOPAS offers advanced facilities for complex geometry handling (e.g., apertures, compensators, dosimetry devices), material settings, definition of physics processes, graphic interfaces, detailed source modeling, and the feasibility of simulating time-dependent aspects of a proton therapy, all managed through a user-friendly parameter system. Thus, TOPAS allows the simulation of full 4D particle therapy systems without the knowledge of Geant4 or advanced programming skills. Details about the TOPAS system are given in Refs. 32–34.

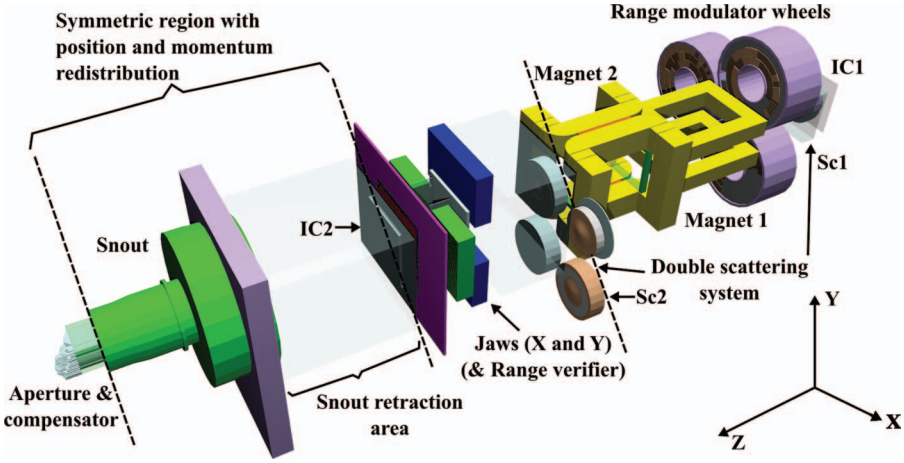

FIG. 1. Treatment head at one gantry at the FHBPTC. The beam enters from the right. Dotted lines show the position of the split planes: upstream of the second scatterer (Sc2), at the second ionization chamber (IC2), and immediately upstream of the field specific aperture.

II.B. The treatment head

The treatment head at one of the gantries at the FHBPTC was simulated in detail using TOPAS, as depicted in Fig. 1. The geometrical setup, and physical processes are described in Refs. 25, 26, and 32–35. At the FHBPTC the gantry settings are divided into eight options, each covering a particular range and modulation width. We have selected fields from options 1, 3, 6, and 8 (two fields for the latter; see Table I). PHSPs were generated and recorded in IAEA format for each of these five options downstream of a squared aperture, no compensator was included. Subsequently the PHSPs were used to compute the deposited dose in a water phantom of $18 \times 18 \times 38.9$ cm^3 divided into $90 \times 90 \times 194$ voxels. The water phantom was embedded in a Lexan tank with 0.5 cm thick walls on all six sides. In all simulations the maximum step size for protons in the water filled tank was set to 0.5 mm.

II.C. Patient geometries

The TOPAS system allows one to track particles on a patient geometry based on CT data in an easy and efficient way. Details on the implementation of CT geometries in TOPAS can be found in Refs. 32 and 34. Two CT patient geometries were considered to compare the effect of the simulations with variance reduction: head and prostate. One field of 10.04 cm of modulation and 12.5 cm of range was used to irradiate the head patient. The head patient consists of an array of $512 \times 512 \times 76$ voxels with dimensions of $0.781 \times 0.781 \times 2.5$ mm^3. The prostate patient consists on an array of $512 \times 512 \times 119$ voxels with dimensions of $0.9 \times 0.9 \times 2.5$ mm^3. For the prostate calculation one field of 11.65 cm of modulation and 27.3 cm of range was used. In both cases the PHSPs were stored downstream the respective compensator. The deposited dose was calculated in each of the two patients from PHSPs simulated with and without variance reduction. The comparison between dose distributions in the patients was made by means of the gamma index test using the 2% and 2 mm criteria[36] for all voxels with a dose value greater than 2% of the maximum value.

TABLE I. Proton beam configuration options used in the study for calculating dose distributions in water. These options cover the minimum and maximum proton ranges deliverable at the MGH gantry treatment heads.

Option	Range (cm)	Modulation width (cm)
A1	5.2	3.0
A3	8.46	6.0
A6	17.57	6.0
A8_1	25.73	6.0
A8_2	27.30	11.65

II.D. The geometrical particle splitting technique

The strategy is to split the primary and secondary protons at strategic locations within the treatment head prior to scoring PHSP. As a consequence the tracking time of the new, split protons for volumes upstream of the splitting position is saved. If the splitting is done in a cylindrically symmetric region, the spatial and momentum distributions of the new protons are distributed symmetrically. This will lead to a decreased correlation in the particle tracks, reducing the number of source particles needed to achieve the required accuracy and statistical uncertainty. To further save time, unnecessary proton splitting is avoided by calculating the direction of the proton prior to splitting, then playing Russian roulette on particles that point outside of a user-defined region of interest. This reduces calculation time compared to the technique used in conventional radiotherapy implementations,[4] where the split is done for all particles, and all secondaries must have their new direction calculated prior to playing Russian roulette on them. The appropriate technique is different for proton therapy than conventional therapy because at clinical energies the average angle of the trajectory of scattered protons is much lower than that of the bremsstrahlung photons or scattered electrons of conventional therapy.

To implement the geometrical split technique, the treatment head was divided by two planar boundaries

perpendicular to the beam axis, one immediately downstream of the second ionization chamber (for setting 1) or immediately upstream of the second scatterer (for setting 2), the other immediately upstream of the aperture, shown in Fig. 1. In setting 1, a proton with significant probability of contributing to the scoring region that reaches a splitting plane is split, i.e., N_s protons are generated from the incident proton; otherwise, it is subject to Russian roulette with a probability of discarding the particle equal to $1 - 1/N_s$, with the weight of the particles that are retained increased accordingly. Henceforth the number of split particles per source proton will be referred as the split number. The position and momentum of each new proton is distributed to N_s different locations randomly rotated with respect to the z-axis, with the weight adjusted by a factor of $1/N_s$. This approach is analogous to a previously published method for conventional radiotherapy.[8,37] For setting 2, protons are subject to a conventional split once they reach the first boundary, i.e., there is no redistribution of position and momentum. However, redistribution of position and momentum is applied at the second plane for both settings. The splitting of all protons at boundaries was achieved by utilizing the so-called parallel geometries in Geant4.[38] This configuration allows to split the protons even at boundaries that are not geometrical boundaries. The tracking of the protons was performed in the standard way for positions off the two boundaries. Particles other than protons are produced in the treatment head and have a negligible effect on dose in the phantom or patient.[18] Thus, for this study, particles different than protons were discarded once created unless stated otherwise to further save time. This should not be done for studies in which secondaries are important, such as secondary neutron dosimetry. The number of primaries used for the simulations of PHSP for dose comparisons is N_p and N_p/N_s^2 for the reference (i.e. all particles were transported and the variance reduction was deactivated) and with variance reduced cases, respectively.

II.E. Computational efficiency

The planar energy fluence of incident protons at the PHSP was used to calculate the statistical uncertainties for each configuration of the treatment head based on a published method.[2,3] The computational efficiency for the production of the PHSP was calculated as[6]

$$\epsilon = \frac{1}{\sigma^2 T}, \tag{1}$$

where σ is an estimation of the statistical uncertainty on the quantity of interest and T is the CPU time to obtain this uncertainty. Here σ^2 was calculated by summing in quadrature the estimated relative uncertainties in all bins with a value greater than 50% of the maximum value.[39] Let us consider only one split plane at the second ionization chamber. The CPU time, T_R, of the reference simulation can be represented as the sum of two times: for the first stage, T_1 represents the time to simulate the protons until the split plane is reached; for the second stage, T_2 represents the time to transport these protons from the first split plane to the PHSP plane, i.e., $T_R = T_1 + T_2$. Analogous to T_R, the CPU time T_S of the simulation with variance reduction can be represented as

$$T_S = T_1 + N_s\, T_2, \tag{2}$$

where N_s is the split number. As N_s increases, the variance will be reduced to

$$\sigma_s^2 = \frac{\sigma_0^2}{N_s}, \tag{3}$$

where σ_0^2 is the variance without variance reduction. By substituting Eqs. (2) and (3) into Eq. (1) with $T_1 = \alpha T_R$ and $T_2 = \beta T_R$ we get

$$\epsilon_s = \frac{\epsilon_0 N_s}{\alpha + \beta\, N_s}. \tag{4}$$

The coefficients α and β represent the fraction of time spent in each stage related to the total time of the simulation without VRT, with $\alpha + \beta = 1$. As expected, the efficiency with variance reduction ϵ_s equals the efficiency of the reference simulation ϵ_0 if $N_s = 1$ and the calculation is N_s times more efficient if the bulk of the time is spent transporting particles to the first split plane ($\alpha \gg \beta\, N_s$). Furthermore, the ratio ϵ_s/ϵ_0 will take the value $1/\beta$ for large values of N_s.

The model is strictly an approximation because it does not consider secondary particles other than protons, however unlike Eq. (1), it gives an estimation of the evolution in the computational efficiency as N_s increases. To evaluate the model in both the reference simulation and the variance reduced simulation, only one split plane was located upstream of Sc2, downstream of IC2 or upstream of the aperture. All efficiency comparisons were made with a 3.1 GHz Intel Xeon processor with Linux operating system. For each scenario 10^5 primary protons were tracked through the treatment head and discarded immediately after they reached the PHSP.

PHSP for dose calculations was generated with a multiprocessor cluster. The cluster consists of 120 processors most of which are 2.66 GHz Intel Xeon with Linux operating system. The TOPAS system allows reuse of the PHSP multiple times; however, in order to test the VRT this option was not used.

To compare the accuracy of the particle splitting technique of the PHSP and dose distributions in the water phantom, the percentage differences of reference simulations as compared to simulation with variance reduction was defined as[7]

$$\Delta^{(i)} = \frac{X_{\mathrm{VRT}}^{(i)} - X_{\mathrm{Ref}}^{(i)}}{X_{\mathrm{Ref}}^{(\mathrm{Max})}}, \tag{5}$$

where $X_{\mathrm{Ref}}^{(i)}$ and $X_{\mathrm{VRT}}^{(i)}$ are the values at bin i from the frequency distribution of the quantity of interest: kinetic energy, planar fluence, angular distribution, mean energy, and profiles of full dose distribution; $X_{\mathrm{Ref}}^{(\mathrm{Max})}$ is the maximum bin value of the quantity in the reference simulation.

III. RESULTS

III.A. Computational efficiency

Figure 2 shows the efficiency for options A1 and A8_1 (Table I) for only one split plane, with the plane situated at

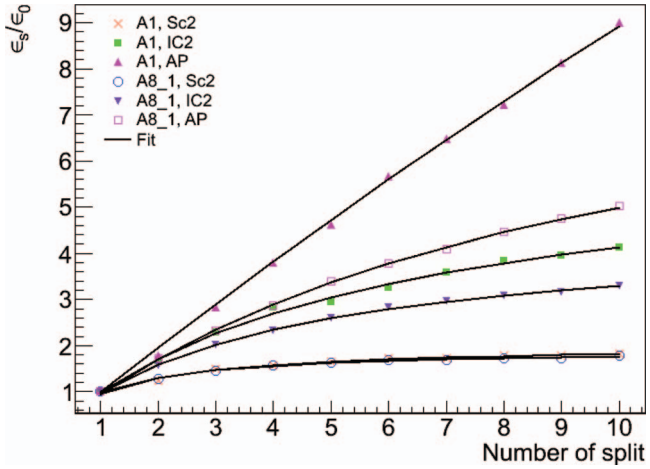

FIG. 2. Normalized efficiency values for a single split plane at the second scatterer (Sc2), the second ionization chamber (IC2), and the aperture (AP) for options A1 and A8_1 (see Table I). The contribution of secondary particles other than protons was discarded for the reference calculation of efficiency. Solid lines represent the fits using Eq. (4).

each of the three positions described above and the curve fitted with Eq. (4). The model describes the shape of the efficiency curve. For option A1 with split plane upstream at Sc2, the coefficients α and β are closer to each other than for the other cases. The coefficients have the values: 0.546 ± 0.064 and 0.497 ± 0.015, respectively, with the maximum gain in efficiency approximately a factor of 2 at the limit for $N_s \gg 10$. In contrast, for $\alpha > \beta$ the gain in efficiency could increase up to 10 at $N_s \gg 10$ for option A8_1 with the split plane upstream of the aperture ($\alpha = 0.965 \pm 0.033$ and $\beta = 0.104 \pm 0.005$).

Figure 3 shows the normalized computational efficiency calculated using Eq. (1). Although a split number bigger than 4 improves the computational efficiency even further for the setting 1, the depth–dose curve and dose profile show significant differences with respect to the reference simulations as shown in Fig. 4 where the same number of protons was scored in the PHSP. The effect is the result of the two split planes being in the same air volume, i.e., the daughter protons are created with a very similar energy as their parents and thus reach the scorer having almost the same energy. Furthermore, the number of primaries for the simulation with variance reduction is reduced to N_p/N_s^2, where N_p is the number of the primaries of the reference simulation. This is because a high split number will require fewer primary protons to reach the same statistical uncertainty.

For setting 2, discrepancies in the depth–dose are reduced (see Fig. 4). The depth–dose curve calculated with a split number of 8 at each split plane agrees with that without the VRT within 1%, with an average difference of (0.2 ± 0.4)%, 1 standard deviation, and a statistical uncertainty in the simulations of 0.3% in the high dose region. However, this placement of the split plane increases the simulation time (see Fig. 4). There is a tradeoff between the targeted accuracy and the time spent to reach a specific accuracy. Therefore, the splitting particle technique should be used with caution.

We found the following setting to work well for the FHBPTC system:

- Apply a split number of 8 upstream of the second scatterer (that is, setting 2 is preferred in this case).
- Apply a split number of 8 upstream of the aperture.
- Discard particles other than protons (results in an additional efficiency gain of a factor of 1.7).
- Apply Russian roulette.

Our resulting efficiency gains range between 10.7 and 24.7 for the different geometrical options. Note that the optimal settings might be different for different configurations of treatment heads.

III.B. Phase space analysis

All simulations were run until approximately 800 000 protons/cm^2 at the phase space plane were created. The planar fluence and the mean energy were estimated by dividing the PHSP into concentric rings of equal area in order to get a description of the spatial and spectral distribution. Figure 5 shows the planar fluence and the mean energy for option A3 with a split number of 8 per split plane and a squared aperture of 8×8 cm. Angular distribution of the incident particles and the spectral distribution are shown in Fig. 6 considering

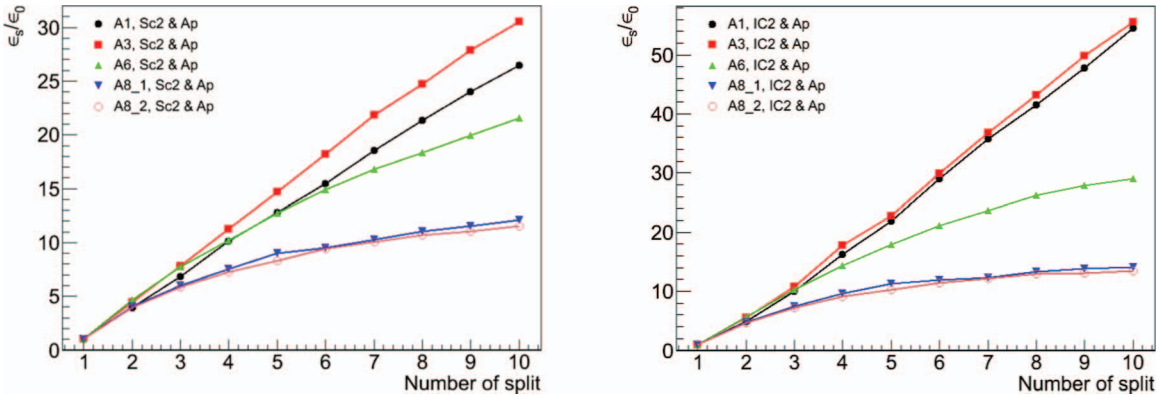

FIG. 3. Normalized efficiency versus the number of splits for the two proposed settings. (Left) Setting 2: Upstream of the second scatterer (Sc2) and upstream of the aperture (Ap). (Right) Setting 1: Downstream of the second ionization chamber (IC2) and upstream of the aperture. Normalization was done with respect to the simulation without variance reduction. Five different geometrical setups (options; labeled as A1 to A8_2) were considered as described in Table I.

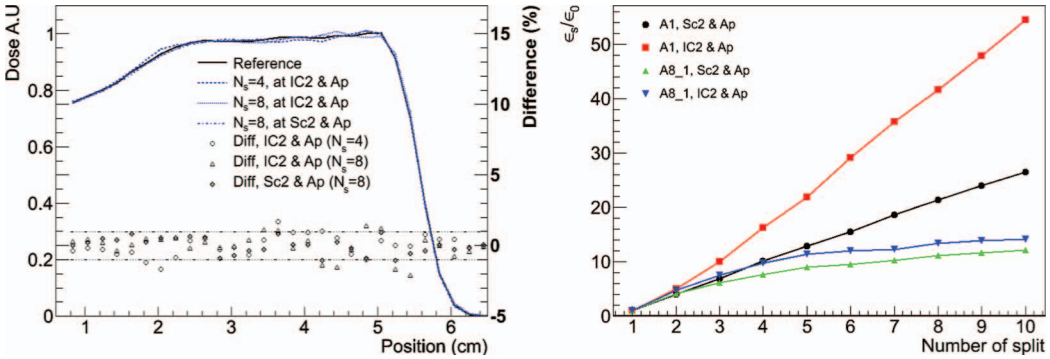

FIG. 4. (Left) Effect on dose profiles by varying the split number for option A1. The difference from the reference curve (no splitting) is also shown, with the difference scale on the right side of the plot. (Right) Decrease in the efficiency due to the first split plane located upstream of the second scatterer (Sc2) rather than downstream of the second ionization chamber (IC2), with the second split plane located upstream of the aperture (Ap) (see Fig. 3).

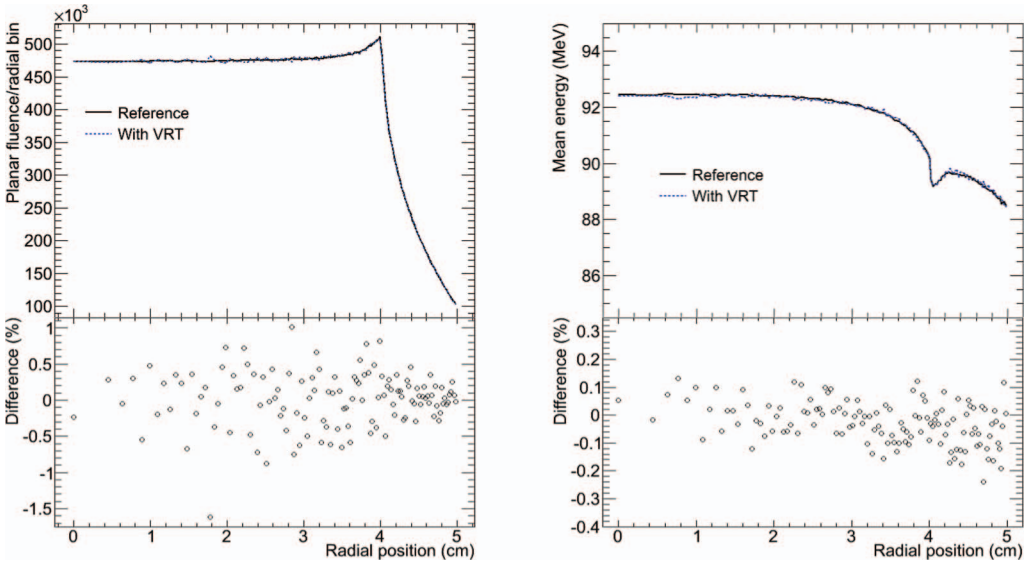

FIG. 5. Planar fluence (left and top) and mean energy (right and top) per radial position for option A3 for the reference simulation (solid) and with variance reduction (dotted). The PHSP was divided into rings of equal area with a maximum radius of 5 cm to consider the penumbra of the beam. The dip at 4 cm in the mean energy is caused by the squared aperture (8 cm side). Relative differences in percent are shown at the bottom for both figures.

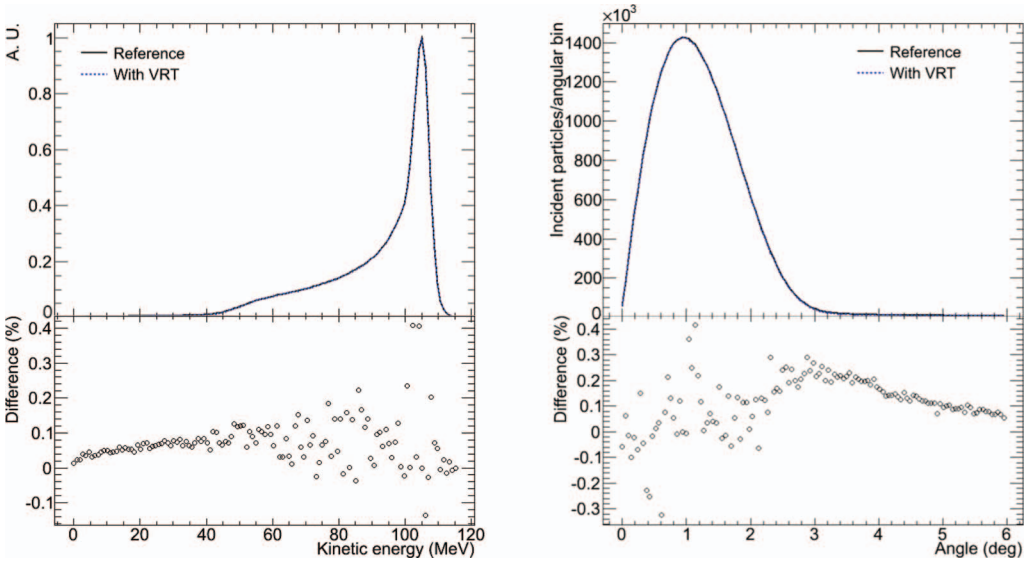

FIG. 6. Energy spectrum (left and top) and angular distribution (right and top) for option A3. Reference simulation (solid) and simulation with variance reduction (dotted) are shown. Their relative differences in percent are shown at the bottom of the plots.

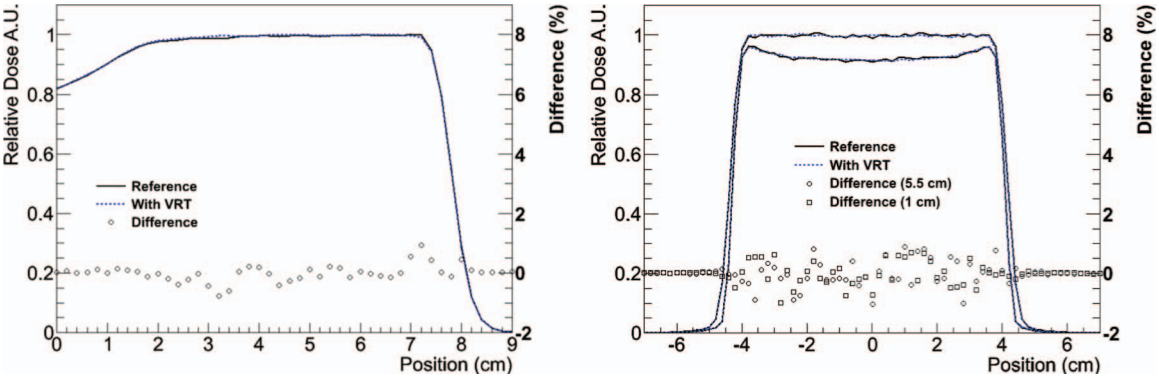

FIG. 7. Depth–dose profile (left) and lateral dose profile at 5.5 cm and at 1 cm from the entrance of the water phantom for option A3. Percentage differences also are shown on the right axis.

angular bins and energy bins of equal size. The planar fluence has differences up to 1.6% compared to the reference simulation, with an average difference of (0.4 ± 0.5)% and a statistical uncertainty of 0.3%. The mean energy has a maximum difference of 0.24%, an average difference of (0.12 ± 0.21)%, and a statistical uncertainty of 0.10%. The energy spectrum has a maximum difference of 0.41% with a statistical uncertainty of 0.18% in the region of the peak. The angular distribution has a maximum difference of 0.42% with a statistical uncertainty of 0.27% in the region of the peak. The average times per CPU of the produced PHSP for all configurations considered are given in Table II.

III.C. Comparison of dose profiles

Full 3D-dose distributions in a water phantom were calculated from the PHSP files and lateral dose profiles as well as depth–dose profiles for all treatment options were obtained. Figures 7 and 8 show the comparison of dose profiles for options A3 and A8_1, respectively. All profiles were normalized with respect to the maximum of the corresponding SOBP. The PHSP generated resulted in statistical fluctuations lower than 1.5% from the maximum of the transverse dose profiles in the SOBP region. The dose distributions had statistical uncertainties of 0.4% in the high dose region. In all cases, percentage differences below 2% (standard deviation in the difference of 0.6%) were reached for the full dose distributions between the reference simulations and the simulations using variance reduction.

TABLE II. Average simulation times per CPU, efficiency and normalized efficiency per CPU for the reference simulations and the simulations using variance reduction for the production of PHSP. The normalization was made with respect to the reference simulations. The planar energy fluence from a bin of 1 cm radius was considered to calculate the variance. The statistical uncertainty of the full PHSPs is on average lower than 0.2% for all options.

		Time (min)		Efficiency (mm^2/MeV s)		Efficiency gain
Option	CPUs	Ref	VRT	Ref	VRT	VRT
A1	250	595.2	32.5	15.4	296.3	19.2
A3	250	592.1	29.7	12.1	245.7	20.3
A6	120	586.0	36.6	57.9	1062.0	18.3
A8_1	90	554.1	57.0	300.7	3017.2	10.0
A8_2	90	592.4	57.1	106.8	1139.1	11.7

III.D. Patient calculations

To evaluate the performance of the geometrical splitting in a clinical situation, dose distributions were calculated for two patients (head and prostate treatments) based on patient CT data.[26] Dose comparison were performed by means of gamma index tests with 2% and 2 mm criteria.[36]

III.D.1. Head treatment field

The average time per CPU (150 were used) for the generation of the PHSP was 585 min per field when simulating without our new splitting technique but only 28 min for the simulation with VRT switched on. Figure 9 shows the transverse dose distribution of the head treatment and the corresponding gamma index map for voxels with dose larger than 2% of the maximum dose. For the full 3D dose distribution, 98.9% of voxels had a gamma value lower than unity.

III.D.2. Prostate treatment field

The average simulation time per CPU (90 were used) for the generation of PHSP for the reference simulation was 587 min per field. When variance reduction is switched on the average simulation time per CPU was only 40 min. Figure 10 shows the coronal view of the dose distributions for both simulations. The corresponding gamma index map for those voxels with dose larger than the 2% of the maximum dose is also shown. The percentage of voxels with gamma value lower than unity is 99.7% by using a 2% with 2 mm criteria.

IV. DISCUSSION

In this work, an implementation and validation of the geometrical based split particle technique in the new TOPAS simulation toolkit was accomplished. PHSPs from simulations

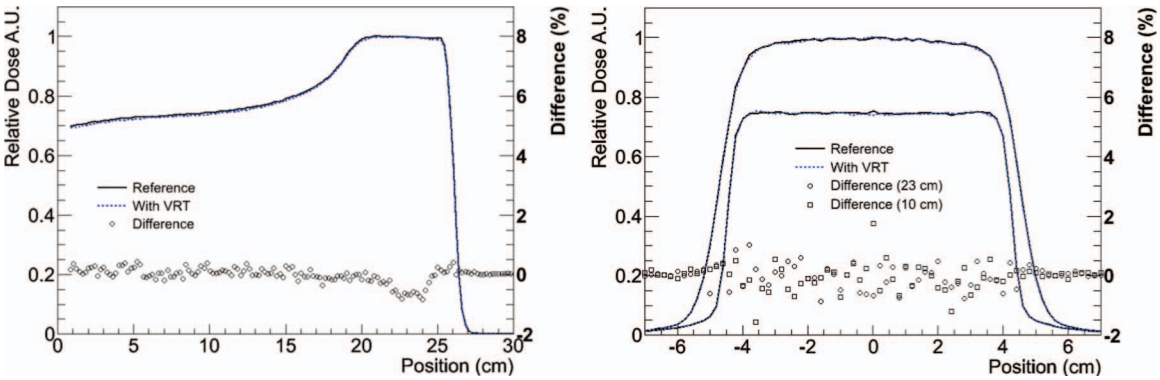

FIG. 8. Depth–dose profile at depth (left) and lateral dose profile (right) at 23 cm and at 10 cm from the entrance of the water phantom for option A8_1. Percentage differences below of 2% also are shown on the right axis.

with and without variance reduction of five configurations of the treatment head at FHBPC were used to analyze the computational efficiency. Analysis of the PHSP was performed, and direct comparison of planar fluences, mean energies, angular distribution, and energy spectrum was made. The efficiency and accuracy of the technique were demonstrated using patient cases.

In the past, several efforts have been made to reduce the Monte Carlo simulation time for the treatment head in proton therapy.[23,27,28] Preliminary data on using a weight window technique in MCNPX nozzle simulations revealed that the simulation time could be reduced by about half,[23] which is a smaller gain than the one reported in our work. The results presented in our work offer the first detailed quantification of the computational efficiency gain when using VRT in Monte Carlo simulations of PHSPs for proton therapy in passive scattering mode. Others have applied a geometrical split (GS) to study the low-dose envelope from scanned pencil beams in a water tank, but the reduction in time between reference and variance reduced simulations was not reported.[27,28] In a different approach, Yepes *et al.*[19] compared MCNPX, Geant4, and a track-repeating algorithm for patient dose calculations. While they did apply a GS to MCNPX, they did not quantify the variance reduction or efficiency gain.

The clinical relevance of this work relies on the fact that potential efficiency gains can be reached without loss in accuracy. It has been stated that the quality assurance of routine IMRT and IMPT treatments is expected to yield >90% agreement for 3% and 3 mm criteria in Gamma analysis (values of 99% have been reported when using MCNPX as a reference).[40] Our results (with 2% and 2 mm criteria) showed better agreement even in more stringent values as in stereotactic surgery, in which it is expected >95% for 3% and 3 mm criteria.

Even a small loss in precision when using VRT's might be acceptable because of the significant difference between Monte Carlo and standard pencil beam based dose calculations.[25,41] Efficiency gains are highly relevant given the fact that TOPAS, including our VRT implementation, is presently in use for patient dose calculations at the Massachusetts General Hospital.

Finally, only the geometrical based particle split and Russian roulette were studied in this work. Further simulation time can be saved by using the PHSP multiple times (an

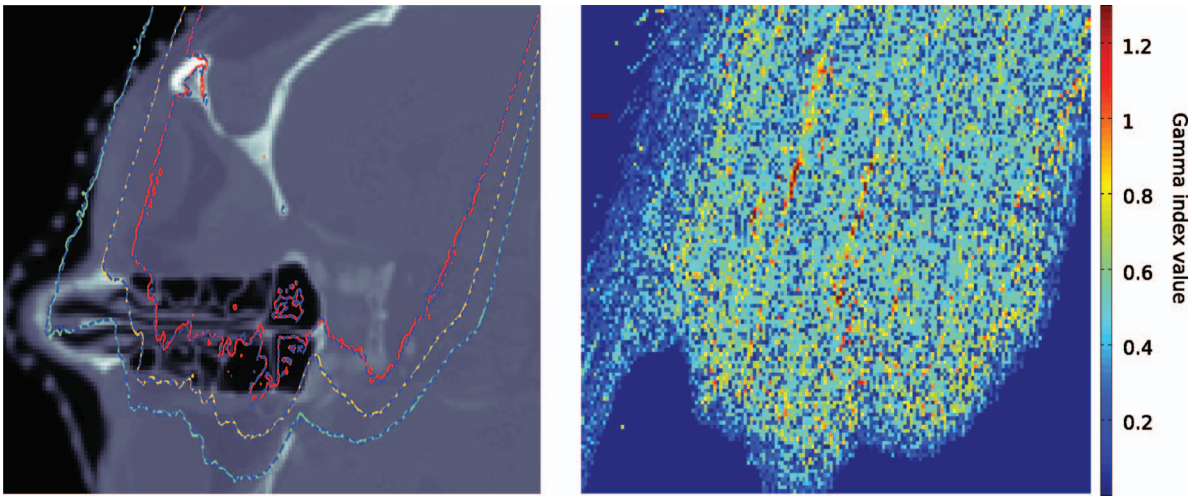

FIG. 9. Transverse view for a head treatment. Reference simulation (solid) and with variance reduction (dotted) are shown in the same image. The right side shows the gamma test values. The percentage of total voxels with a gamma value lower than unity is 98.9% by using a 2 mm and 2% criteria.

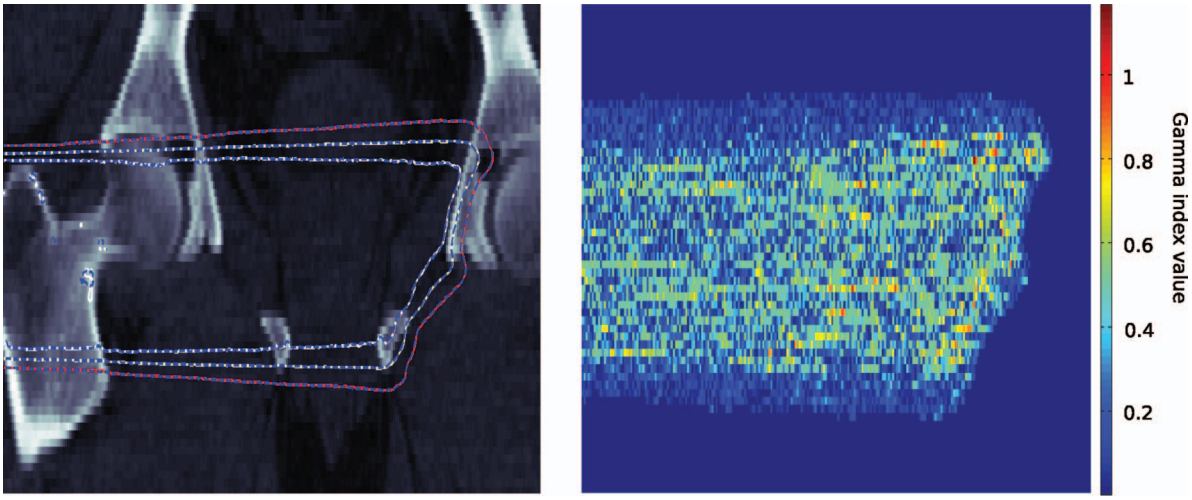

FIG. 10. Coronal view for a prostate case. (Left) Reference simulation (solid) and with variance reduction (dotted) are shown. The right side shows the gamma test values. The percentage of total voxels with a gamma value lower than unity is 99.7% by using a 2 mm and 2% criteria.

option implemented in TOPAS), and by choosing an adequate energy or range cutoff. This work offers a good starting point for continued research on adapting VRT to the specific needs of proton therapy in passive scatter mode.

V. SUMMARY AND CONCLUSIONS

A geometrical variation of the split particle technique for proton therapy was adapted and validated for TOPAS, a new Geant4 Monte Carlo simulation application, in this case used for tracking protons through the treatment head of one of the gantries at the Francis H Burr Proton Therapy Center. By considering the cylindrically symmetric region of the treatment head and the splitting planes separated at strategic positions, a considerable time saving was achieved without compromising the precision of the calculated quantities (dose, fluence, etc.). With a split number of 8, with Russian roulette and by killing particles other than protons, this approach reduced the time for PHSP simulations for clinical MC dose calculation at FHBPTC by a factor of 10–20. A simple model for the computational efficiency was developed to describe its performance when the number of split protons is increased.

Fluence and dose distributions in homogeneous and nonhomogeneous volumes calculated using particle splitting were well within clinical tolerance of the results of reference simulations done without particle splitting.

The method can be adopted for other proton Monte Carlo codes or other treatment head designs in passive scattering mode.

ACKNOWLEDGMENTS

J.R.M. acknowledges the Consejo Nacional de Ciencia y Tecnología (México) and H. Salazar-Ibargüen (Benemérita Universidad Autónoma de Puebla) for financial supporting for his visit to the Massachusetts General Hospital. J.R.M. thanks J. Shin (University of California San Francisco) for discussions on Geant4 topics. This work was supported by National Institutes of Health/National Cancer Institute (NIH/NCI) under R01 CA 140735-01.

[a]Electronic mail: joserm84@gmail.com

[1]M. Goitein, *Radiation Oncology: A Physicist's-Eye View* (Springer, New York, 2008).
[2]I. Chetty, B. Curran, J. E. Cygler, J. J. DeMarco, G. Ezzell, B. A. Faddegon, I. Kawrakow, P. J. Keall, H. Liu, C. Ma, D. W. O. Rogers, J. Sauntjens, D. Sheikh-Bagheri, and J. V. Siebers, "Report of the AAPM Task Group No. 105: Issues associated with clinical implementation of Monte Carlo-based photon and electron external beam treatment planning," Med. Phys. **34**, 4818–4853 (2007).
[3]C.-M. Ma, J. S. Li, T. Pawlicki, S. B. Jiang, J. Deng, M. C. Lee, T. Koumrian, M. Luxton, and S. Brain, "A Monte Carlo dose calculation tool for radiotherapy treatment planning," Phys. Med. Biol. **47**, 1671–1690 (2002).
[4]I. Kawrakow, D. W. O. Rogers, and B. R. B. Walters, "Large efficiency improvements in BEAMnrc using directional splitting," Med. Phys **31**, 2883–2898 (2004).
[5]L. Brualla, F. Salvat, and R. Polanco-Zamora, "Efficient Monte Carlo simulation of multileaf collimators using geometry-related variance-reduction techniques," Phys. Med. Biol. **54**, 4345–4360 (2009).
[6]M. Fragoso, I. Kawrakow, B. Faddegon, T. Solberg, and I. Chetty, "Fast, accurate photon beam accelerator modeling using BEAMnrc: A systematic investigation of efficiency enhancing methods and cross-section data," Med. Phys. **36**, 5451–5466 (2009).
[7]F. Hasenbalg, M. Fix, E. Born, R. Mini, and I. Kawrakow, "VMC++ versus BEAMnrc: A comparison of simulated linear accelerator heads for photon beams," Med. Phys. **35**, 1521–1531 (2008).
[8]J. Sempau, A. Badal, and L. Brualla, "A PENELOPE-based system for the automated Monte Carlo simulation of clinacs and voxelized geometries-application to far-from-axis fields," Med. Phys. **38**, 5887–5895 (2011).
[9]A. Bielajew and W. Rogers, *Variance-Reduction Techniques in Monte Carlo Transport of Electrons and Photons* (Plenum, New York, 1998), pp. 407–419.
[10]I. Kawrakow and B. R. B. Walters, "Efficient photon beam dose calculations using DOSXYZnrc with BEAMnrc," Med. Phys. **33**, 3046–3056 (2006).
[11]L. Grevillot, T. Frisson, D. Maneval, N. Zahara, J.-N. Badel, and D. Sarrut, "Simulation of a 6 MV Elekta Precise Linac photon beam using GATE/Geant4," Phys. Med. Biol. **56**, 903–918 (2011).
[12]R. D. Lewis, S. J. S. Ryde, D. A. Hancock, and C. J. Evans, "An MCNP-based model of a linear accelerator X-Ray beam" Phys. Med. Biol. **44**, 1219–1230 (1999).
[13]H. P. Smith and J. C. Wagner, "A case study in manual and automated Monte Carlo variance reduction with a deep penetration reactor shielding problem," Nucl. Sci. Eng. **149**, 23–37 (2005).

[14]R. H. Olsher, "A practical look at Monte Carlo variance reduction methods in radiation shielding," Nucl. Eng. Technol. **38**, 225–230 (2006).
[15]T. Booth, "A sample problem for variance reduction in MCNP," Los Alamos National Laboratory New Mexico report, LA-10363-MS, 1985.
[16]P. D. Soran, D. C. McKeon, and T. E. Booth, "Calculation of Monte Carlo importance functions for use in nuclear-well logging calculations," IEEE. Trans. Nucl. Sci. **37**, 936–942 (1990).
[17]J. C. Wagner and A. Haghighat, "Automated variance reduction of Monte Carlo shielding calculations using the discrete ordinates adjoint function," Nucl. Sci. Eng. **128**, 186–208 (1998).
[18]H. Paganetti, "Nuclear interactions in proton therapy: Dose and relative biological effect distributions originating from primary and secondary particles," Phys. Med. Biol. **47**, 747–764 (2002).
[19]P. Yepes, S. Randeniya, P. Taddei, and W. Newhauser, "Monte Carlo fast dose calculator for proton radiotherapy: Application to a voxelized geometry representing a patient with prostate cancer," Phys. Med. Biol. **54**, N21–N28 (2009).
[20]P. Yepes, S. Randeniya, P. Taddei, and W. Neuhauser, "A track-repeating algorithm for fast Monte Carlo dose calculations of proton radiotherapy," Nucl. Technol. **168**, 736–740 (2009).
[21]M. Fippel and M. Soukup, "A Monte Carlo dose calculation algorithm for proton therapy," Med. Phys. **31**, 2263–2273 (2004).
[22]J. Li, B. Shahine, E. Fourkal, and C.-M. Ma, "A particle track-repeating algorithm for proton beam dose calculation," Phys. Med. Biol. **50**, 1001–1010 (2005).
[23]W. Newhauser, J. Fontenot, Y. Zheng, J. Polf, U. Titt, N. Koch, X. Zhang, and R. Mohan, "Monte Carlo simulations for configuring and testing an analytical proton dose-calculation algorithm," Phys. Med. Biol. **52**, 4569–4584 (2007).
[24]X. Jia, J. Schümann, H. Paganetti, and S. B. Jiang, "GPU-based fast Monte Carlo dose calculation for proton therapy," Phys. Med. Biol. **57**, 7783–7797 (2012).
[25]H. Paganetti, H. Jiang, S.-Y. Lee, and H.-M. Kooy, "Accurate Monte Carlo simulations for nozzle design, commissioning and quality assurance for a proton radiation therapy facility," Med. Phys. **31**, 2107–2118 (2004).
[26]H. Paganetti, H. Jiang, K. Parodi, R. Slopsema, and M. Engelsman, "Clinical implementation of full Monte Carlo dose calculation in proton beam therapy," Phys. Med. Biol. **53**, 4825–4853 (2008).
[27]G. O. Sawakuchi, U. Titt, D. Mirkovic, G. Ciangaru, X. R. Zhu, N. Sahoo, M. T. Gillin, and R. Mohan, "Monte Carlo investigation of the low-dose envelope from scanned proton pencil beams," Phys. Med. Biol. **55**, 711–721 (2010).
[28]G. O. Sawakuchi, D. Mirkovic, L. A. Perles, N. Sahoo, X. R. Zhu, G. Ciangaru, K. Suzuki, M. T. Gillin, R. Mohan, and U. Titt, "An MCNPX Monte Carlo model of a discrete spot scanning proton beam therapy nozzle," Med. Phys. **37**, 4960–4970 (2010).
[29]J. Fan, W. Luo, E. Fourkal, T. Lin, J. Li, I. Veltchev, and C.-M. Ma, "Shielding design for a laser-accelerated proton therapy system," Phys. Med. Biol. **52**, 3913–3930 (2007).
[30]K. Parodi, A. Ferrari, F. Sommerer, and H. Paganetti, "Clinical CT-based calculations of dose and positron emitter distributions in proton therapy using the FLUKA Monte Carlo code," Phys. Med. Biol. **52**, 3369–3387 (2007).
[31]W. Newhauser, N. Koch, S. Hummel, M. Ziegler, and U. Titt, "Monte Carlo simulations of a nozzle for the treatment of ocular tumors with high-energy proton beams," Phys. Med. Biol. **50**, 5229–5249 (2005).
[32]J. Perl, J. Shin, J. Schümann, B. Faddegon, and H. Paganetti, "TOPAS an innovative proton Monte Carlo platform for treatment head and patient simulations in research and clinical applications," Med. Phys. **39**, 6818–6837 (2012).
[33]J. Shin, J. Perl, J. Schümann, H. Paganetti, and B. Faddegon, "A modular method to handle multiple time-dependent quantities in Monte Carlo simulations," Phys. Med. Biol. **57**, 3295–3308 (2012).
[34]J. Schümann, H. Paganetti, J. Shin, B. Faddegon, and H. Paganetti, "Efficient voxel navigation for proton therapy dose calculation in TOPAS and Geant4," Phys. Med. Biol. **57**, 3281–3293 (2012).
[35]C. Z. Jarlskog and H. Paganetti, "Physics settings for using the Geant4 toolkit in proton therapy," IEEE. Trans. Nucl. Sci. **55**, 1018–1025 (2008).
[36]D. Low, W. Harms, S. Mutic, and J. Purdy, "A technique for the qualitative evaluation of dose distributions," Med. Phys. **25**, 656–661 (1998).
[37]K. Bush, S. Zavgorodni, and W. Beckham, "Azimuthal particle redistribution for the reduction of latent phase-space variance in Monte Carlo simulation," Phys. Med. Biol. **52**, 4345–4360 (2007).
[38]J. Apostolakis, M. Asai, G. Cosmo, A. Howard, V. Ivanchenko, and M. Verderi, "Parallel geometries in Geant4: Foundation and recent enhancements," IEEE Nucl. Sci. Symp. Conf. Rec. **NSS 08**, 883–886 (2008).
[39]D. W. O. Rogers, and R. Mohan, "Questions for comparison of clinical Monte Carlo codes," in *Proceedings of the 13th ICCR*, edited by T. Bortfeld, and W. Schlegel (Springer-Verlag, Berlin, 2000), pp. 120–122.
[40]U. Titt, B. Bednarz, and H. Paganetti, "Comparison of MCNPX and Geant4 proton energy deposition predictions for clinical use," Phys. Med. Biol. **57**, 6381–6393 (2012).
[41]H. Paganetti, "Range uncertainties in proton therapy and the role of monte carlo simulations," Phys. Med. Biol. **57**, R99–R117 (2012).